PCCP

ROYAL SOCIETY OF CHEMISTRY

PAPER

View Article Online
View Journal | View Issue

Cite this: *Phys. Chem. Chem. Phys.*, 2026, **28**, 9691

Formation and transfer of HCl in a macromolecular noncovalent complex: does the roaming atom mechanism play a role?

Min Liu, †[a] Marwa Abdelmouleh,[a] Alexandre Giuliani,[bc] Laurent Nahon[b] and Jean-Christophe Poully *[a]

Received 20th December 2025,
Accepted 27th March 2026

DOI: 10.1039/d5cp04965b

rsc.li/pccp

In the last twenty years, the "roaming atom" mechanism emerged and gained enormous interest thanks to its success in explaining experimental results that are not accounted for by the widely accepted statistical transition state theory. However, despite intense efforts for describing this new mechanism, intriguing questions remain. A crucial one is: does it play a role in molecular systems larger than 25 atoms, in particular those relevant to life sciences and pharmacology? Here, we present data on HCl transfer within a noncovalent complex built upon vancomycin, an antibiotic containing more than 170 atoms, and a tripeptide, following UV-VUV photoabsorption in the gas phase. In this molecular system, the experimental energetics of HCl formation is incompatible with the values obtained by quantum-chemical calculations, assuming a straightforward mechanism governed by the transition state. Instead, our results are consistent with a roaming mechanism.

1. Introduction

The widely accepted statistical transition state theory has been very successful in describing and quantifying the energetics and kinetics of chemical reactions involving the cleavage and formation of covalent and/or noncovalent bonds. However, in the last twenty years, the so-called "roaming atom" mechanism emerged and gained tremendous interest, owing to the failure of transition state theory to explain intriguing experimental results, mostly obtained on gas-phase neutral molecules undergoing either unimolecular reactions after photoabsorption, or bimolecular reactions by collision with another neutral species.[1] These experimental findings stimulated theoretical developments that managed to rationalize experimental data, pushing forward researches on this new field. In the roaming atom mechanism, on the pathway from reactants to products of a given chemical reaction, there is no tight transition state, defined as a saddle point on the potential-energy surface (PES) of the system. Instead, the roaming atom (or group of atoms) explores large and relatively flat regions of the PES, bypassing saddle points. Along its trajectory, "frustrated bonds" between the roaming species and other atoms of the system are successively formed and cleaved.[2]

A crucial characteristic is the low total energy (kinetic, internal and potential) required for the roaming atom mechanism to play a major role, once the roaming radical is formed. For instance, it largely dominates in the 30–60 kcal mol^{-1} (1.3–2.6 eV) range for Cl roaming and H abstraction from acetylene, following collision between a chlorine atom and acetylene in the gas phase.[3] As recently pointed out by Mauguière *et al.*,[4] the total energy is a phase-space criterion, and "the manifestation of flat regions of the PES in phase space provides a natural dynamical definition of the roaming region". Another characteristic of the roaming atom mechanism is the asymmetric energy partitioning between the reaction products: for instance, after absorption of one 308 nm photon by acetaldehyde, CH_3 roams and abstracts H from HCO, forming vibrationally highly-excited CH_4 and cold CO.[5]

Up to now, the roaming atom mechanism has only been reported in relatively small molecular systems, with tyrosine (24 atoms) being among the largest one.[6] The authors of a gas phase UV photofragmentation study found that the role of the "roaming atom" mechanism strongly increases from formaldehyde (H_2CO) to propionaldehyde (C_2H_5CHO), and suggest that it should also be the case for larger aliphatic aldehydes.[7] In his recent review, A. G. Suits[2] supports this conclusion and makes it even more general, noting that as the system becomes larger, the density of states increases considerably thereby opening the

[a] *CIMAP UMR 6252 Université Caen Normandie, ENSICAEN, CNRS, CEA, Normandie Univ, 14070 Caen, France. E-mail: poully@ganil.fr*
[b] *Synchrotron SOLEIL, 91190 Saint Aubin, France*
[c] *INRAE, UAR1008, Transform Department, Rue de la Géraudière, 44316 Nantes, France*
† Current address: Department of Rehabilitation Medicine, The Seventh Affiliated Hospital of Sun Yat-sen University, Shenzhen, Guangdong 518107, P. R. China.

route for increased roaming interactions. However, the experimental techniques used hitherto to identify the roaming atom mechanism do not allow studying much larger systems. Indeed, previous studies reported the asymmetric energy partitioning of the reaction products as experimental evidence of roaming, obtained by vibrational or rotational spectroscopy of gas-phase neutral molecules.[5,7–10] The latter were brought in the gas phase thanks to resistive heating, which inherently limits the size of the target species because of thermally-induced chemical decomposition at a temperature below that required for vaporization.

Recently, we proposed a new method to record the UV-VUV spectrum of thermally fragile neutral molecules in the gas phase using charge-tagging action spectroscopy, which consists in recording the photofragmentation yield of the molecular system as a function of wavelength, using mass spectrometry.[11] Our test case was vancomycin, an antibiotic containing over 170 atoms, brought intact into the gas phase by electrospray ionization, a soft technique able to vaporize and ionize fragile species such as thermolabile species and noncovalent complexes. Here, we apply the same experimental strategy to test the roaming atom mechanism in the same system, providing direct evidence of HCl formation and intermolecular transfer in a vancomycin–tripeptide noncovalent complex after UV photoabsorption. We also give phase space arguments strongly supporting a roaming process.

2. Results and discussion

2.1. Formation of HCl from vancomycin and transfer to the tripeptide

First, let us focus on the $[V+R-2H]^{2-}$ noncovalent complex composed of deprotonated vancomycin (noted $[V-H]^{1-}$) and deprotonated $Ac_2{}^{L}K^{D}A^{D}A$ (noted $[R-H]^{1-}$), a tripeptide mimicking the natural receptor of vancomycin (see the chemical structure of this complex in Fig. 1). In the mass spectra of the $[V+R-2H]^{2-}$ complex after photoabsorption at low photon energy (4.5–7.5 eV), numerous peaks due to product anions are observed (see Fig. 2a). The most abundant at 6.5 eV photon energy is $[V+R-2H-CO_2]^{1-}$, which is formed by single electron detachment followed by CO_2 loss from vancomycin: it has already been observed for photoabsorption of the same precursor ion at higher photon energies,[12] but also of doubly-deprotonated vancomycin and other multiply-deprotonated peptides.[11,13] It might seem unusual to observe the cleavage of a covalent bond without dissociation of the noncovalent complex, but one has to keep in mind the high binding energy of vancomycin–$Ac_2{}^{L}K^{D}A^{D}A$ as well as the low photon energy (4.77 eV for angiotensin) required for CO_2 loss from radicals created by single electron detachment from doubly-deprotonated peptides.[13] Moreover, loss of CO_2 from the carboxylate group of vancomycin can occur without disrupting the H-bond network between vancomycin and $Ac_2{}^{L}K^{D}A^{D}A$ (see Fig. 1). Nonetheless, we also observe the expected process of noncovalent bond breaking: it gives rise to the intense peaks present around m/z 371 in the mass spectra of $[V+R-2H]^{2-}$ (*cf.* Fig. 2a) and assigned to $[R-H]^{1-}$, based on the very good agreement between simulated and experimental isotopic patterns that are mainly due to the natural abundance of ^{13}C (see Fig. 2b).

Interestingly, peaks of weaker intensity also appear around m/z 407: they have never been reported in previous mass spectrometry studies on noncovalent complexes between V and R, to the best of our knowledge. Isotopic pattern analysis supports the assignment of these peaks to $[R-H+HCl]^{1-}$ (see Fig. 2c). Another observation makes this assignment sounder: the presence of $[V-H-HCl]^{1-}$ in the same mass spectra (see Fig. 2a). Indeed, in the absence of electron detachment, $[V-H-HCl]^{1-}$ and $[R-H+HCl]^{1-}$ are released as complementary fragment ions by dissociation of the precursor $[V+R-2H]^{2-}$. This

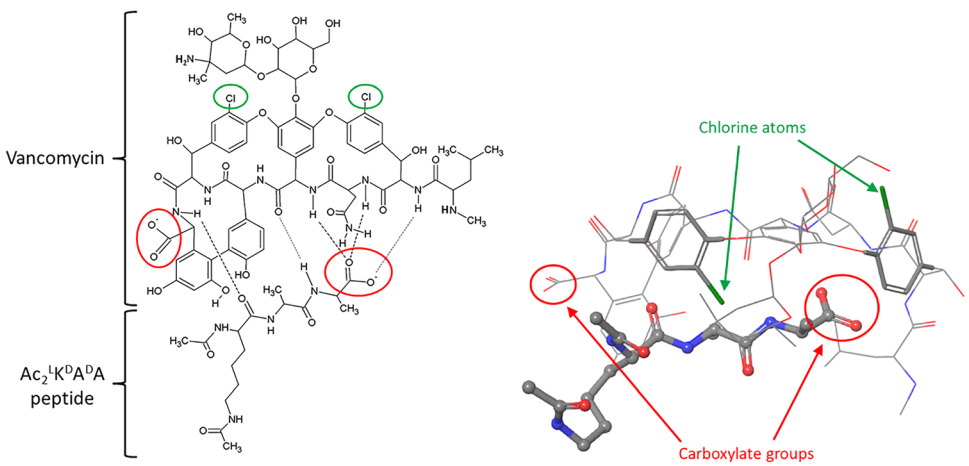

Fig. 1 Left: chemical structure of $[V+R-2H]^{2-}$ in the gas phase. The H bonds linking vancomycin and $Ac_2{}^{L}K^{D}A^{D}A$ are highlighted in dashes. Carboxylates and chlorines are encircled in red and green, respectively. Right: 3D molecular structure of the vancomycin–$Ac_2{}^{L}K^{D}A^{D}A$ noncovalent complex in a crystal (PDB ID: 1FVM). Chlorines are shown in green and indicated by green arrows, oxygens in red, nitrogens in blue, carbons in grey, and hydrogens are omitted for clarity. $Ac_2{}^{L}K^{D}A^{D}A$ is depicted with balls and tubes and vancomycin with lines (the substituted chlorophenyl groups are highlighted with thicker lines).

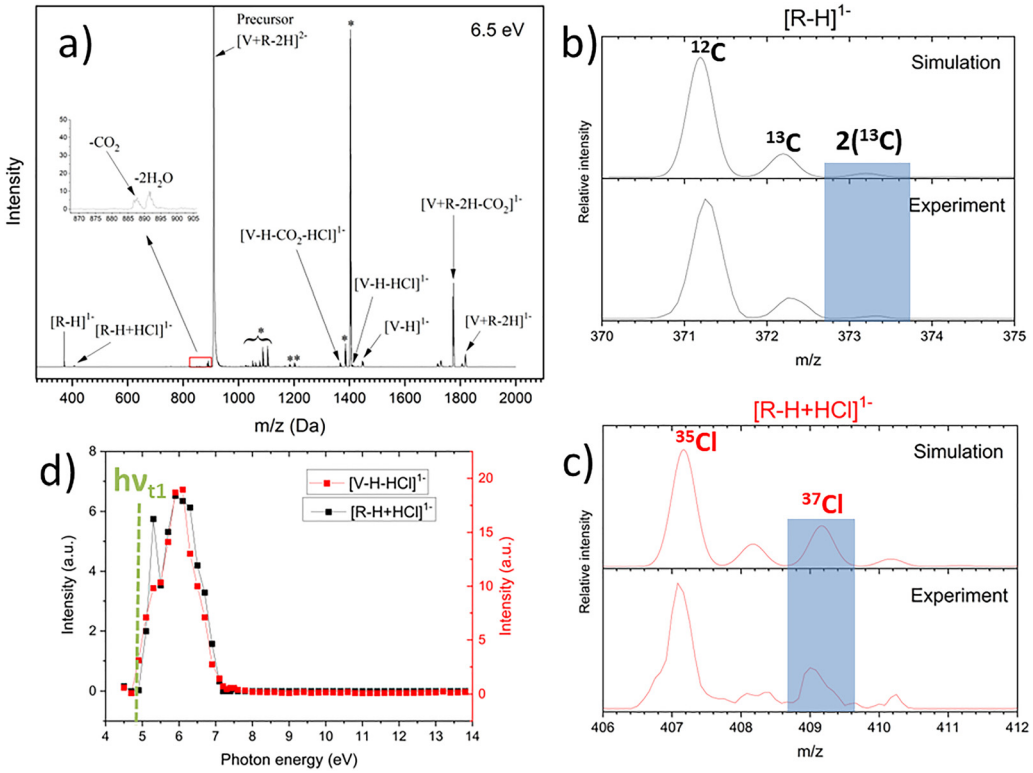

Fig. 2 (a) Experimental mass spectrum of $[V + R-2H]^{2-}$ after photoabsorption at 6.5 eV (* indicates background peaks. The most intense one around *m/z* 1400 is due to collision-induced dissociation of $[V + R-2H]^{2-}$ in the trap). (b) and (c) Zoom into two different regions corresponding to $[R-H]^{1-}$ and $[R-H + HCl]^{1-}$, respectively, and comparison with isotopic pattern simulations. (d) Evolution of the yield corresponding to the complementary fragments $[R-H + HCl]^{1-}$ and $[V-H-HCl]^{1-}$ as a function of photon energy.

conclusion is further confirmed by the remarkably similar yields of these two complementary anions over the whole photon energy range 4.5–13.8 eV (see Fig. 2d). In addition, both yields drop close to zero above 7 eV, where electron detachment dominates and triggers alternative relaxation channels. Furthermore, the yield of $[R-H+HCl]^{1-}$ is about half that of $[V-H-HCl]^{1-}$, which can be rationalized by looking at the geometrical structure of the vancomycin–$Ac_2{}^{L}K^{D}A^{D}A$ complex (see Fig. 1): two chlorine atoms are bound to phenyl moieties in vancomycin, but only one can plausibly be transferred to $Ac_2{}^{L}K^{D}A^{D}A$ owing to its orientation towards the peptide.

Hence, we find that HCl formation within $[V+R-2H]^{2-}$ is triggered by UV photoexcitation, and occurs together with dissociation of the complex and transfer of HCl to $[R-H]^{1-}$. This is a remarkable observation for several reasons. First, HCl is the only molecular fragment observed to bind $[R-H]^{1-}$, even though H_2O and CO_2 are also lost from vancomycin within $[V+R-2H]^{2-}$ in the same photon energy range (*cf.* Fig. 2a). Second, to our knowledge, no previous work mentions the transfer of a molecular fragment between ligand and receptor after photofragmentation of a gas phase molecular noncovalent complex. Third, HCl is most probably H-bound to $[R-H]^{1-}$ within $[R-H+HCl]^{1-}$, because addition of H + Cl to organic molecules requires a C=C bond that is absent from $[R-H]^{1-}$. One could argue that $[R-H+HCl]^{1-}$ might actually be $[R+Cl]^{1-}$, formed after proton transfer followed by Cl^- transfer from vancomycin to Ac_2KAA, but it is very unlikely because Cl^- release from a neutral chlorobenzene group of vancomycin is much higher in energy than homolytic bond cleavage forming a chlorine radical. Furthermore, we also observed previously abundant loss of HCl from $[V+R-H]^-$, $[V-2H]^{2-}$ and $[V-H]^-$.[11] Thus, we assume that $[R-H+HCl]^{1-}$ is a noncovalent complex. The survival of such a weakly bound species over the 100 ms trapping timescale is unexpected after absorption of one photon of 5–7 eV energy, because formation of $[R-H+HCl]^{1-}$ requires cleavage of the H bonds between vancomycin and $Ac_2{}^{L}K^{D}A^{D}A$ (see Fig. 1) that is thought to proceed after intramolecular vibrational energy redistribution, which should also cleave the H bond between $[R-H]^{1-}$ and HCl. Therefore, $[R-H+HCl]^{1-}$ must be produced with negligible excess vibrational energy.

2.2. Energetics of the formation of HCl within vancomycin

In this section, we aim at describing the energetics of the following reaction:

$$[V+R-2H]^{2-} \rightarrow [R-H+HCl]^{1-} + [V-H-HCl]^{1-} \quad (1)$$

Let us investigate the first step, namely HCl formation within vancomycin. Given the chemical structure of the two groups carrying chlorines in vancomycin (*cf.* Fig. 1), it is natural to consider the UV irradiation of neutral chlorobenzene.

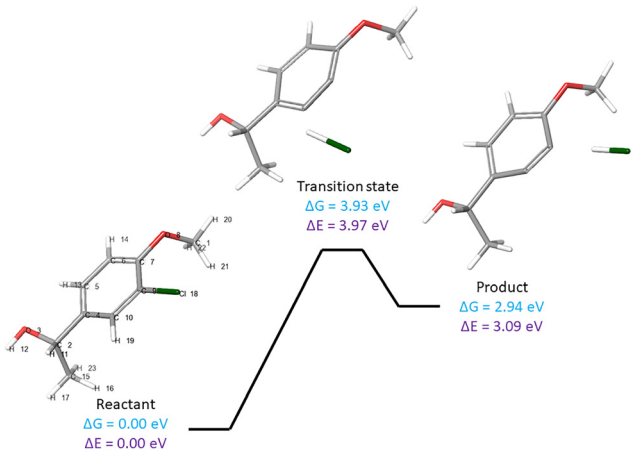

Fig. 3 Scheme of the HCl formation by the "direct abstraction" mechanism in molecular model 1 of vancomycin. Carbon, hydrogen, oxygen and chlorine atoms are depicted in grey, white, red and green, respectively. ΔE and ΔG stand for zero-point corrected energy at 0 K and free energy at 300 K, respectively, calculated at the B3PW91/aug-cc-pVTZ level and relative to the reactant.

Interestingly, HCl emission from thick films of chlorobenzene under UV irradiation at 248 nm (5.0 eV) and low fluences has been reported,[14] as well as from isolated chlorobenzene after UV (266 nm, 4.7 eV) photoexcitation in the gas phase.[15] The authors of the latter study report a calculated value of 3.8–4.0 eV for the potential energy barrier corresponding to a mechanism involving direct abstraction of the closest H by Cl, compatible with their experimental data. In vancomycin, such H atoms are present in the substituted chlorophenyl groups.

We have checked, by means of quantum-chemical calculations on the model system of vancomycin depicted in Fig. 3 at the same theory level as the one employed in the study on chlorobenzene,[15] that the substitutions only marginally alter the energy diagram for the "direct abstraction" mechanism (see Fig. 3), with a transition state around 4 eV and a product around 3 eV. This product is a noncovalent complex with a weakly-bound HCl, thus if we assume that the same mechanism occurs in $[V+R-2H]^{2-}$, HCl transfer to $Ac_2{}^{L}K^{D}A^{D}A$ within $[V+R-2H]^{2-}$ should require little energy and give the resulting $[R-H+HCl]^{1-}$—$[V-H-HCl]^{1-}$ noncovalent complex. Therefore, we include a similar energy diagram in Fig. 4 to account for HCl formation from vancomycin within $[V+R-2H]^{2-}$, followed by HCl transfer to $Ac_2{}^{L}K^{D}A^{D}A$.

In the last paragraph, we have obtained a value of 3 eV for the energy corresponding to HCl formation by the direct abstraction mechanism in a simplified molecular model of vancomycin, by means of quantum-chemical calculations (see Fig. 3). Now, let us estimate the experimental value of this energy from our data. The second step of reaction (1) is dissociation of the noncovalent bonds between vancomycin and $Ac_2{}^{L}K^{D}A^{D}A$ to give the two complementary anions $[R-H+HCl]^{1-}$ and $[V-H-HCl]^{1-}$. The corresponding dissociation energy E_{D1} is estimated below. Given the flexible structure of the $Ac_2{}^{L}K^{D}A^{D}A$ tripeptide as well as the Coulomb repulsion of the product anions, we include a reverse potential energy barrier for this step in the diagram of Fig. 4. Fig. 2d shows that the threshold photon energy for the formation of $[R-H+HCl]^{1-}$ and $[V-H-HCl]^{1-}$ from $[V+R-2H]^{2-}$ is $h\nu_{t1} \approx 4.8$ eV: we assume that this energy corresponds to the highest barrier in the diagram of Fig. 4. Thus, we obtain the following equation giving $E_F(HCl)$, the energy involved in the formation of HCl in vancomycin:

$$E_F(HCl) = h\nu_{t1} - E_{D1}$$

Now, let us estimate E_{D1} from another reaction (2) undergone by $[V+R-2H]^{2-}$:

$$\begin{aligned}[V+R-2H]^{2-} &\rightarrow [(V-H-CO_2)\cdots(R-H)]^{2-}+CO_2\\ &\rightarrow [(V-2H-CO_2)\cdots R]^{2-}+CO_2\\ &\rightarrow [(V-CO_2)-2H]^{2-}+R+CO_2\end{aligned} \quad (2)$$

The first step is loss of CO_2 without dissociation of the noncovalent complex, which is only possible if CO_2 is lost from vancomycin, because the carboxylate group of $Ac_2{}^{L}K^{D}A^{D}A$ shares three strong H-bonds with vancomycin (see Fig. 1). We expect negligible rearrangement of the products here, and thus no reverse barrier for step 1 in the energy diagram of Fig. 4 (right). The second step is proton transfer from vancomycin to

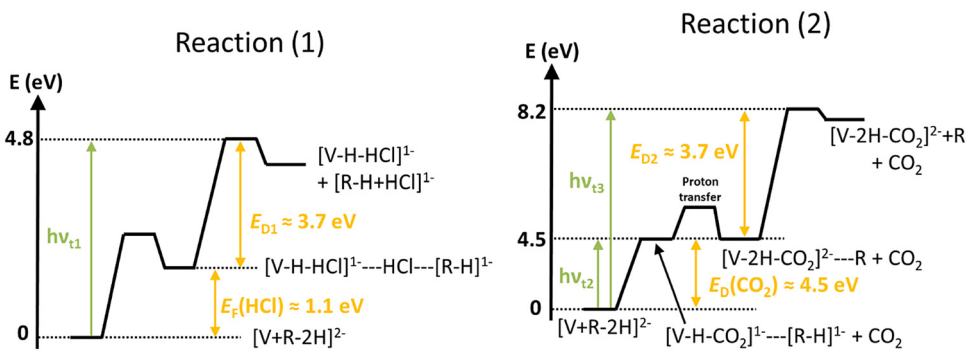

Fig. 4 Proposed potential energy diagrams of reactions (1) and (2). Experimental energy values E_X for the different reaction steps are given and experimental threshold photon energies are indicated as $h\nu_{tx}$.

the most basic site of $Ac_2{}^{L}K^{D}A^{D}A$, which is the carboxylate group. This proton transfer probably occurs from one of the amide groups engaged in H bonds with the carboxylate group. Finally, dissociation of the noncovalent bonds between vancomycin and $Ac_2{}^{L}K^{D}A^{D}A$ gives $[V–2H–CO_2]^{2-}$ and neutral $Ac_2{}^{L}K^{D}A^{D}A$, with a reverse barrier lower than for reaction (1) because of the absence of Coulomb repulsion. Looking at the diagram of Fig. 4, we obtain:

$$E_{D2} \approx h\nu_{t3} - h\nu_{t2}$$

We can obtain $h\nu_{t3}$ and $h\nu_{t2}$ from our experimental threshold photon energies shown in Fig. S1. We can also assume that $E_{D1} \approx E_{D2}$, because the noncovalent interactions between vancomycin and $Ac_2{}^{L}K^{D}A^{D}A$ within $[V+R–2H]^{2-}$ are similar before and after proton transfer: the number of H bonds is five and they involve a deprotonated group. Hence, we get:

$$E_{D1} \approx h\nu_{t3} - h\nu_{t2} \approx 8.2 - 4.5 \approx 3.7 \text{ eV}$$

It is important to note that the same value of 3.7 eV is obtained from our data on the $[V+R–H]^{1-}$ precursor ion, following the same method (see Fig. S2). This value is higher than the reported binding energy of 40.3 kcal mol^{-1} (1.75 eV) from surface induced dissociation experiments,[16] which is due to the significant rearrangement expected after dissociation. In addition, dissociation of this complex requires a large entropy increase at 300 K, resulting from cleavage of the five strong H bonds that constrain the conformation of the receptor in the binding pocket of vancomycin.[17] We can now calculate E_F(HCl) (*cf.* Fig. 4):

$$E_F(\text{HCl}) = h\nu_{t1} - E_{D1} \approx 4.8 - 3.7 \approx 1.1 \text{ eV}$$

This value of E_F(HCl) = 1.1 eV is far lower than the 3 eV obtained by our quantum-chemical calculations for the direct abstraction mechanism (see Fig. 3). Moreover, the barrier for HCl production cannot exceed $h\nu_{t1} \approx 4.8$ eV, not much higher than the value obtained from our calculations (see Fig. 3). An important consequence is the expected presence of this process in other related systems in the same photon energy range, which is indeed the case for $[V+R–H]^{-}$, $[V–2H]^{2-}$ and $[V–H]^{-}$.[11] For $[V+R–H]^{1-}$, HCl loss even dominates at low photon energy, in the same range as for $[V+R–2H]^{2-}$.

2.3. Possible mechanisms explaining HCl formation and transfer

In this section, we explore the possible mechanisms that could account for our unexpected observations regarding HCl formation and intermolecular transfer within the vancomycin–$Ac_2{}^{L}K^{D}A^{D}A$ complex.

In the previous section, we have mentioned a study where isolated chlorobenzene has been found to release HCl after UV photoabsorption, following a mechanism where Cl directly abstracts the neighboring H.[15] The same mechanism in the substituted chlorobenzene groups of vancomycin has similar energetics, according to our quantum-chemical calculations on molecular model 1: in particular, the energy of the product is about 3 eV above that of the reactant (see Fig. 3). This is strongly different from our experimental results for the vancomycin–$Ac_2{}^{L}K^{D}A^{D}A$ complex, where this energy is estimated to be 1.1 eV. The much lower energy of the $[R–H]^{1-}$—HCl—$[V–H–HCl]^{1-}$ product might in principle be explained by a higher binding energy of HCl compared to the model system of Fig. 3, due to an additional H bond involving $Ac_2{}^{L}K^{D}A^{D}A$, but even a strong H bond cannot account for the 1.9 eV difference. We have calculated, at the same level of theory, the energy of the product corresponding to abstraction of either H_{13} or H_{14} in the model shown in Fig. 3: it is even 0.3–0.4 eV higher than abstraction of the closest H (H_{19}). Thus, we believe that a major rearrangement of vancomycin has occurred after HCl formation. This rearrangement could involve the formation of a new covalent bond between carbon atoms, if the chlorine atom abstracts a hydrogen of another phenyl ring: let us assume that the chlorine belonging to the C-terminal chlorophenyl group abstracts the closest H of the central phenyl group. We explored this hypothesis by performing quantum-chemical calculations on molecular model 2 shown in Fig. 5. Optimization of the geometry of the reactant only very slightly modifies the initial geometry from vancomycin. Furthermore, after removal of H and Cl, geometry optimization (without any constraint) leads to the formation of a C–C covalent bond and an additional ring in between the two phenyl rings. Our calculations also reveal that the energy of the product is about 1 eV below that of the reactant, confirming the high stabilization due to the large rearrangement of the molecular system. Deeper investigation is however needed to unambiguously identify the H atom abstracted by Cl.

In the previous paragraph, we have shown that our experimental energetics may be explained by abstraction of a hydrogen by chlorine followed by HCl formation and covalent bond formation within vancomycin. Then, according to our

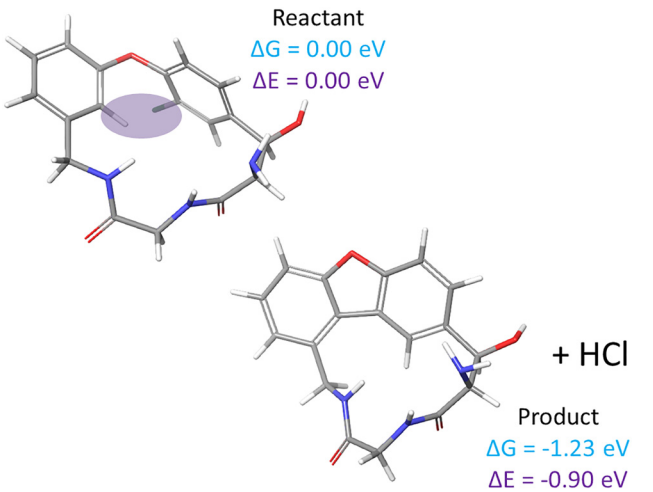

Fig. 5 Structure and energy of the reactant and product of HCl formation within molecular model 2 of vancomycin. ΔE and ΔG stand for zero-point corrected energy at 0 K and free energy at 300 K, respectively, calculated at the B3PW91/6-31+g(d,p) level and relative to the reactant.

experimental results (see Section 2.1), $[R–H+HCl]^{1-}$ is released, which implies that HCl is transferred to $Ac_2{}^{L}K^{D}A^{D}A$ and the noncovalent bonds between vancomycin and $Ac_2{}^{L}K^{D}A^{D}A$ are cleaved. However, the order of these events is not known *a priori*. Usually, dissociation of a noncovalent complex is explained by the presence of excess vibrational energy, which can be due to internal conversion after photoabsorption. Here, the surprising observation is the detection of a noncovalently-bound complex between HCl and $Ac_2{}^{L}K^{D}A^{D}A$ after photoabsorption in the whole 4.5–7 eV photon energy range, with a probability that rises first (see Fig. 2d). This indicates that the increasing difference between the photon energy and the energy of the $\{[R–H+HCl]^{1-} + [V–H–HCl]^{1-}\}$ product (see Fig. 4) is not converted into excess vibrational energy of $[R–H+HCl]^{1-}$. Thus, most of this energy must be taken away by $[V–H–HCl]^{1-}$: such an asymmetric energy partitioning is not encountered in statistical reactions. Instead, it is typical of roaming reactions, where the roaming atom or fragment usually contains a high amount of internal energy (rotational or/and vibrational). However, it is not the case in the reaction $CH_2CHC(O)Cl \rightarrow HCl + CO + HC_2H$ triggered by photoabsorption at 193 nm, where Cl roams before abstracting H and forming an internally cold HCl.[8] Here, the signature of roaming is found not only in the asymmetric energy partitioning, but also in the atypical motion of the reactive Cl: in order to abstract H and then be transferred to $Ac_2{}^{L}K^{D}A^{D}A$, either the Cl pointing towards $Ac_2{}^{L}K^{D}A^{D}A$ has to move back and forth, or the Cl pointing away has to travel at least 6 Å (see Fig. 1). Note that other examples of Cl roaming reactions involving creation of HCl have been reported.[3,18–20]

3. Conclusion

HCl formation and transfer from vancomycin to $Ac_2{}^{L}K^{D}A^{D}A$ is observed in a noncovalent complex after UV photoabsorption in the gas phase, followed by dissociation of the complex. Our experimental results show that the energetics for HCl formation is unusually low, as compared to a direct abstraction mechanism governed by the transition state, which energy budget has been evaluated by quantum chemistry calculations. Strikingly, we observe an asymmetric internal energy partitioning between the released product anions. Furthermore, the mechanism for HCl formation and transfer implies atypical motion of the reactive Cl. We believe that only a roaming atom mechanism can account for these observations. To our knowledge, vancomycin is by far the largest molecule to date where this mechanism is found to play a role. Our results provide a benchmark for future theoretical investigation, not only on HCl loss from molecules, but more broadly on the roaming atom mechanism itself. Moreover, they also raise intriguing questions, for instance whether this mechanism is common in biological molecular systems, and even dominant in some cases. If confirmed, the latter hypothesis could deeply modify currently accepted views in chemistry in general, and biochemistry in particular.

4. Methods

4.1. Experiments

Vancomycin hydrochloride and $Ac_2{}^{L}K^{D}A^{D}A$ have been purchased from Sigma-Aldrich as powders of over 80% purity, and used without further purification. Electrospray solutions have been prepared in 50 : 50 (volume ratio) water/methanol at 50 μM concentration with 1% of ammonia to deprotonate the molecules. The UV-VUV gas phase tandem mass spectrometry experiments were performed using a commercial mass spectrometer (Thermo Finnigan LTQ XL) coupled to the DESIRS beamline at the SOLEIL synchrotron radiation facility.[21] The set-up has previously been described in detail,[22] only a brief description is given here. The molecular ions were brought in the gas phase from the solution by electrospray ionization using a syringe pump with a flow rate of about 5 μL min^{-1} and a needle biased at 5 kV in front of a capillary held at 35 V. Ions were then guided through a quadrupole and an octopole, before being injected, thermalized by helium buffer gas and trapped in a commercial linear triple quadrupole ion trap. In this trap, the ions of interest were selected by mass-to-charge ratio (m/z) with an isolation width of 6–10 mass units depending on the ion. After isolation, the ions were irradiated by photons from the DESIRS VUV beamline of the SOLEIL synchrotron facility in Saint-Aubin (France).[21] Product anions from photoabsorption as well as remaining precursors were then analyzed with respect to m/z in the ion trap, and these mass spectra were accumulated until sufficient statistics was reached (typically 30 spectra).

Mass spectra were recorded for different photon energies, using 0.2 eV steps between 4.5 and 7.5 eV and between 7.2 and 13.8 eV. The UV/VUV beam was free of high harmonics owing to the use of a Kr gas filter (7.2–13.8 eV) and a quartz window (4.5–7.5 eV). The photon flux was in the 10^{12}–10^{13} photons per s range and was measured independently using an AXUV100 photodiode (international radiation detectors) under the measurement conditions. The total number of photons for a given ion and energy was tuned to obtain a maximum of 10% conversion of the precursor ions to photoproducts, in order to limit the occurrence of sequential two-photon processes. It was regulated by adjusting the exit slit (100–600 μm) of the monochromator and a mechanical shutter that controlled the irradiation time of the trapped ions between 200 and 1000 ms.

Results were obtained in the form of one mass spectrum for each photon energy. To quantify the formation of photoproducts as a function of photon energy, action spectra were constructed. These spectra show the yield of each photoproduct as a function of photon energy. This yield has been calculated from the intensity of the peaks in the mass spectra, corrected for the number of incident photons (to account for photon flux variations upon scanning) and for the precursor ion intensity (to account for fluctuations of the number of precursor ions in the ion trap). The yield of photoproduct A can thus be calculated for a given photon energy according to the following:

$$I_{A(rel)} = \frac{I_A}{I_{pre} \cdot N_{phot}}$$

where I_A is the abundance of photoproduct A, measured by the sum of the peak intensities of all isotopes. I_{pre} is the abundance of the precursor ion peak (sum of all isotopes). The incident number of photons N_{phot} is given by:

$$N_{phot} = \Phi_q \cdot \Delta t \cdot \frac{w_{exp}}{w_{ref}}$$

where Φ_q is the photon flux measured in the reference scan with the photodiode, Δt is the irradiation time, w_{exp} is the slit width during the experiment, and w_{ref} is the slit width during the reference scan.

4.2. Calculations

All calculations were performed using the Gaussian 09 package[23] with the B3PW91 functional and the aug-cc-pVTZ or 6-31+g(d,p) basis sets. Geometry optimization was carried out with the default Berny algorithm for the reactant and transition state, but we used the GDIIS algorithm for the product of model 1. Atoms 1, 6, 7 and 8 (see Fig. 3) were frozen during optimization of model 1 in order to retain the geometrical constraints present in vancomycin. Vibrational frequencies were calculated to confirm the absence of negative frequencies for minima of the potential energy surface (reactant and product), and the presence of a single negative frequency (-438 cm^{-1}) for the transition state, confirming a first-order saddle point. This frequency calculation also allowed the potential energy to be corrected by the vibrational zero-point energy and the Gibbs free energy at 300 K to be calculated.

Conflicts of interest

There are no conflicts of interest to declare.

Data availability

Supplementary information includes fragment ion yields as a function of photon energy, for $[V+R-2H]^{2-}$ and $[V+R-H]^{1-}$ precursors. See DOI: https://doi.org/10.1039/d5cp04965b.

Data for this article, including mass spectra of negative ions produced from doubly-deprotonated vancomycin–Ac2KAA produced by UV photoabsorption in the 4.5–7 eV range, are available at Zenedo at https://doi.org/10.5281/zenodo.17936105.

References

1 J. M. Bowman and B. C. Shepler, *Annu. Rev. Phys. Chem.*, 2011, **62**, 531–553.
2 A. G. Suits, *Annu. Rev. Phys. Chem.*, 2020, **71**, 77–100.
3 Y. Bai, Y.-L. Fu, J. Qi, L. Liu, X. Lu, Y.-C. Han, D. H. Zhang and B. Fu, Exclusive roaming mechanism for the Cl + C2H2 → C2H + HCl bimolecular reaction, *Nat. Commun.*, 2025, **16**, 2732.
4 F. A. L. Mauguière, P. Collins, Z. C. Kramer, B. K. Carpenter, G. S. Ezra, S. C. Farantos and S. Wiggins, *Annu. Rev. Phys. Chem.*, 2017, **68**, 499–524.
5 B. R. Heazlewood, M. J. T. Jordan, S. H. Kable, T. M. Selby, D. L. Osborn, B. C. Shepler, B. J. Braams and J. M. Bowman, Roaming is the dominant mechanism for molecular products in acetaldehyde photodissociation, *Proc. Natl. Acad. Sci. U. S. A.*, 2008, **105**, 12719–12724.
6 J. Westermayr, M. Gastegger, D. Vörös, L. Panzenboeck, F. Joerg, L. González and P. Marquetand, Deep learning study of tyrosine reveals that roaming can lead to photodamage, *Nat. Chem.*, 2022, **14**, 914–919.
7 P.-Y. Tsai, K.-C. Hung, H.-K. Li and K.-C. Lin, Photodissociation of Propionaldehyde at 248 nm: Roaming Pathway as an Increasingly Important Role in Large Aliphatic Aldehydes, *J. Phys. Chem. Lett.*, 2014, **5**, 190–195.
8 P.-W. Lee, P. G. Scrape, L. J. Butler and Y.-P. Lee, Two HCl-Elimination Channels and Two CO-Formation Channels Detected with Time-Resolved Infrared Emission upon Photolysis of Acryloyl Chloride [CH2CHC(O)Cl] at 193 nm, *J. Phys. Chem. A*, 2015, **119**, 7293–7304.
9 D. Townsend, S. A. Lahankar, S. K. Lee, S. D. Chambreau, A. G. Suits, X. Zhang, J. Rheinecker, L. B. Harding and J. M. Bowman, The Roaming Atom: Straying from the Reaction Path in Formaldehyde Decomposition, *Science*, 2004, **306**, 1158–1161.
10 M. L. Hause, N. Herath, R. Zhu, M. C. Lin and A. G. Suits, Roaming-mediated isomerization in the photodissociation of nitrobenzene, *Nat. Chem.*, 2011, **3**, 932–937.
11 M. Liu, M. Abdelmouleh, A. Giuliani, L. Nahon and J.-C. Poully, UV–VUV Photofragmentation Spectroscopy of Isolated Neutral Fragile Macromolecules: A Proof-of-Principle Based on a Deprotonated Vancomycin–Peptide Noncovalent Complex, *J. Phys. Chem. A*, 2022, **126**, 9042–9050.
12 M. Abdelmouleh, M. Lalande, V. Vizcaino, T. Schlathölter and J.-C. Poully, Photoinduced Processes within Noncovalent Complexes Involved in Molecular Recognition, *Chem. – Eur. J.*, 2020, **26**, 2243–2250.
13 R. Antoine, L. Joly, A. R. Allouche, M. Broyer, J. Lemoine and P. Dugourd, Electron photodetachment of trapped doubly deprotonated angiotensin peptides. UV spectroscopy and radical recombination, *Eur. Phys. J. D*, 2009, **51**, 117–124.
14 S. Georgiou, A. Koubenakis, J. Labrakis and M. Lassithiotaki, Formation and desorption dynamics of photoproducts in the ablation of van der Waals films of chlorobenzene at 248 nm, *J. Chem. Phys.*, 1998, **109**, 8591–8600.
15 B. Behera and P. Das, HCl elimination in the photolysis of chlorobenzene at 266 nm: An FT-IR spectroscopy and quantum chemical study, *Chem. Phys. Lett.*, 2021, **774**, 138601.
16 Z. Yang, E. R. Vorpagel and J. Laskin, Influence of the Charge State on the Structures and Interactions of Vancomycin Antibiotics with Cell-Wall Analogue Peptides: Experimental and Theoretical Studies, *Chem. – Eur. J.*, 2009, **15**, 2081–2090.
17 J. C. Poully, F. Lecomte, N. Nieuwjaer, B. Manil, J. P. Schermann, C. Desfrancois, F. Calvo and G. Gregoire, Probing the specific interactions and structures of gas-

phase vancomycin antibiotics with cell-wall precursor through IRMPD spectroscopy, *Phys. Chem. Chem. Phys.*, 2010, **12**, 3606–3615.

18 B. Joalland, Y. Shi, A. Kamasah, A. G. Suits and A. M. Mebel, Roaming dynamics in radical addition–elimination reactions, *Nat. Commun.*, 2014, **5**, 4064.

19 C. Foley, S. Alavi, B. Joalland, B. Broderick, N. Dias and A. Suits, Imaging the infrared multiphoton excitation and dissociation of propargyl chloride, *Phys. Chem. Chem. Phys.*, 2019, **21**, 1528–1535.

20 B. Joalland, Y. Shi, A. Estillore, A. Kamasah, A. Mebel and A. Suits, Dynamics of Chlorine Atom Reactions with Hydrocarbons: Insights from Imaging the Radical Product in Crossed Beams, *J. Phys. Chem. A*, 2014, **118**, 9281–9295.

21 L. Nahon, N. de Oliveira, G. A. Garcia, J.-F. Gil, B. Pilette, O. Marcouillé, B. Lagarde and F. Polack, DESIRS: a state-of-the-art VUV beamline featuring high resolution and variable polarization for spectroscopy and dichroism at SOLEIL, *J. Synchrotron Radiat.*, 2012, **19**, 508–520.

22 A. R. Milosavljevic, C. Nicolas, J.-F. Gil, F. Canon, M. Refregiers, L. Nahon and A. Giuliani, *J. Synchrotron Radiat.*, 2012, **19**, 174–178.

23 M. J. Frisch, G. W. Trucks, H. B. Schlegel, G. E. Scuseria, M. A. Robb, J. R. Cheeseman, G. Scalmani, V. Barone, G. A. Petersson, H. Nakatsuji, X. Li, M. Caricato, A. Marenich, J. Bloino, B. G. Janesko, R. Gomperts, B. Mennucci, H. P. Hratchian, J. V. Ortiz, A. F. Izmaylov, J. L. Sonnenberg, D. Williams-Young, F. Ding, F. Lipparini, F. Egidi, J. Goings, B. Peng, A. Petrone, T. Henderson, D. Ranasinghe, V. G. Zakrzewski, J. Gao, N. Rega, G. Zheng, W. Liang, M. Hada, M. Ehara, K. Toyota, R. Fukuda, J. Hasegawa, M. Ishida, T. Nakajima, Y. Honda, O. Kitao, H. Nakai, T. Vreven, K. Throssell, J. A. Montgomery, Jr., J. E. Peralta, F. Ogliaro, M. Bearpark, J. J. Heyd, E. Brothers, K. N. Kudin, V. N. Staroverov, T. Keith, R. Kobayashi, J. Normand, K. Raghavachari, A. Rendell, J. C. Burant, S. S. Iyengar, J. Tomasi, M. Cossi, J. M. Millam, M. Klene, C. Adamo, R. Cammi, J. W. Ochterski, R. L. Martin, K. Morokuma, O. Farkas, J. B. Foresman and D. J. Fox, Gaussian, Inc., Wallingford CT, 2016, **vol. 2016**.

